Decadal freshening of the Antarctic Bottom Water exported from the Weddell Sea

Loïc Jullion, Alberto C. Naveira Garabato, Michael P. Meredith, Paul H. Holland, Peggy Courtois, Brian A. King

Decadal freshening of the Antarctic Bottom Water exported from the Weddell Sea

Loïc Jullion, * Alberto C. Naveira Garabato

University of Southampton, National Oceanography Centre, Southampton, United Kingdom,

Michael P. Meredith,

British Antarctic Survey, Cambridge, United Kingdom

Scottish Association for Marine Science, Oban, U.K.

Paul R. Holland,

British Antarctic Survey, Cambridge, United Kingdom,

Peggy Courtois,

University of Southampton, National Oceanography Centre, Southampton, United Kingdom,

Brian A. King

National Oceanography Centre, Southampton, United Kingdom,

* *Corresponding author address:* Loïc Jullion, Geophysical Fluid Dynamics Institute, Florida State University, Tallahassee, FL 32306, USA

E-mail: l.jullion@fsu.edu

ABSTRACT

Recent decadal changes in Southern Hemisphere climate have driven strong responses from the cryosphere. Concurrently, there has been a marked freshening of the shelf and bottom waters across a wide sector of the Southern Ocean, hypothesised to be caused by accelerated glacial melt in response to a greater flux of warm waters from the Antarctic Circumpolar Current onto the shelves of West Antarctica. However, the circumpolar pattern of changes has been incomplete: no decadal freshening in the deep layers of the Atlantic sector had been observed. In this study, we document a significant freshening of the Antarctic Bottom Water exported from the Weddell Sea, which is the source for the abyssal layer of the Atlantic overturning circulation, and we trace its possible origin to atmospheric-forced changes in the ice shelves and sea ice on the eastern flank of the Antarctic Peninsula that include an anthropogenic component. These findings suggest that the expansive and relatively cool Weddell gyre does not insulate the bottom water formation regions in the Atlantic sector from the ongoing changes in climatic forcing over the Antarctic region.

1. Introduction

Antarctic Bottom Water (AABW), filling the deepest layer of the World's oceans, plays a critical role in the lower limb of the global oceanic overturning circulation, and contributes to the regulation of Earth's climate by storing heat, freshwater and biogeochemical tracers in the abyssal ocean (Orsi et al. 1999). Changes in the properties of AABW or in the strength of its circulation have the potential to impact significantly on the global ocean's energy budget, sea level and the deep ocean ecosystem (Purkey and Johnson 2010; Church et al. 2011; Sutherland et al. 2012).

The properties of AABW are set by interactions between the ocean, the atmosphere and the cryosphere in the margins of Antarctica, and are very sensitive to the drastic and rapid climate changes occurring in the region (Foster and Carmack 1976; Gill 1973; Orsi et al. 1999; Jacobs 2004; Nicholls et al. 2009). Near the continental slope, Warm Deep Water (WDW) originating in the Antarctic Circumpolar Current (ACC) penetrates onto the shelf in certain locations, often in modified form. This mixes with cold shelf waters that are made saline by brine rejection during sea ice formation, creating dense products that spill off the shelf and entrain further mid-layer waters as they descend in plumes (Killworth 1974; Carmack and Foster 1975; Foldvik et al. 2004; Wilchinsky and Feltham 2009). Interaction of shelf waters with the underside of floating ice shelves is also important in setting the properties of some of the shelf waters, with temperatures below the surface freezing point made possible by the pressure at which the interaction occurs (Nicholls et al. 2009).

In the Weddell Sea, the locally-formed variety of AABW is comprised of two water masses, namely Weddell Sea Bottom Water (WSBW) and Weddell Sea Deep Water (WSDW). WSBW, formed primarily in the southern Weddell Sea near Filchner-Ronne Ice shelf (Nicholls et al. 2009), is the coldest and densest of AABW varieties ($\Theta < -0.7°$C, $\gamma_n > 28.31$ kg m^{-3}). WSBW is too dense to overflow the topographic barriers isolating the Weddell Sea from the lower latitude Southern Ocean to the north (Fig 1a). The lighter WSDW ($28.26 < \gamma_n < 28.31$ kg m^3, $0° > \Theta > -0.7°$C) is either produced directly by mixing between dense shelf waters

and WDW (Foldvik et al. 2004; Nicholls et al. 2009), or indirectly by slow diapycnal upwelling of WSBW within the Weddell gyre. The WSDW formed near the Larsen ice shelves (LIS) in the western Weddell Sea (Fig 1b) is generally lighter and fresher than the AABW formed further south (Fahrbach et al. 1995; Gordon et al. 2001; Huhn et al. 2008; Gordon et al. 2010) and is preferentially exported toward the Scotia Sea through several deep gaps in the South Scotia Ridge (Naveira Garabato et al. 2002b).

The occurrence of extensive decadal-scale changes in the bottom layer of the ocean has been reported recently.The abyssal layer of the Southern Hemisphere oceans warmed significantly between the 1980s and the 2000s (Johnson and Doney 2006; Johnson et al. 2008a,b; Purkey and Johnson 2010). Purkey and Johnson (2012) argued that this warming was potentially an indication of a slowdown of the lower limb of the MOC. In the Indian and Pacific sectors of the Southern Ocean, AABW and its precursor shelf waters have been freshening since the 1960s. In the Ross Sea, the shelf and bottom waters have freshened at rates of 0.03 decade^{-1} and 0.01 decade^{-1}, respectively, since 1958 (Jacobs and Giulivi 2010). Off Adélie Land, Aoki et al. (2005) and Rintoul (2007) reported an AABW freshening of 0.03 between the 1990s and the mid-2000s. The origin of the freshening trend in the Indo-Pacific sector of the Southern Ocean has been attributed to an accelerated melting of the ice shelves of West Antarctica (Shepherd et al. 2004; Rintoul 2007; Jacobs et al. 2002; Jacobs and Giulivi 2010), where the proximity of the ACC to the continent allows warm water to flood the coastal areas (Thoma et al. 2008; Jacobs et al. 2011).

In the Weddell Sea, however, no evidence of a freshening of the AABW has thus far been found (Fahrbach et al. 2011). Using 8 hydrographic sections along the Greenwich meridian between 1984 and 2008, Fahrbach et al. (2011) suggested that the WSDW and WSBW in the central Weddell Sea were dominated by multi-annual cycles. This lack of a clear freshening trend has led to the perception of this sector as being largely resilient to the ongoing changes in Southern Hemisphere climate, most likely due to the region's ice shelves being sheltered from the influence of the ACC by the cyclonic Weddell gyre.

Recently, however, model simulations have raised the prospect of potentially rapid changes in the southern Weddell Sea ice shelves in response to atmospheric-driven perturbations in the ocean circulation caused in part by receding sea ice (Hellmer et al. 2012). The realism of the climatic sensitivities of AABW properties apparent in these model results is unclear, but it does call for further detailed understanding of the response of the ocean-ice system in the Atlantic sector to climatic changes in forcing, underpinned by observations.

Here we provide direct evidence that the AABW exported from the Weddell gyre to the lower limb of the Atlantic Meridional Overturning Circulation has been freshening over the last decade, and trace the most likely origin of this freshening to atmospheric-forced ice shelf collapse, deglaciation and sea ice changes on the eastern side of the Antarctic Peninsula. These findings complete the pattern of circumpolar freshening of dense waters of Antarctic origin, but also suggest that the processes driving the freshening in the Atlantic sector are distinct from those in the Indo-Pacific sector.

2. Data

a. The SR1b repeat hydrographic section

Detection and attribution of decadal change in ocean circulation and climate is a foremost problem in global environmental sciences. In the upper ocean, the advent of an array of profiling floats has revolutionised the ability to quantify and understand such changes (Roemmich et al. 2009), but achieving the same in the deep ocean remains a significant challenge. Nowhere is this more true than in the data-sparse Southern Ocean. In this context, the SR1b repeat hydrographic section in Drake Passage (between South America and the tip of the Antarctic Peninsula; Fig.1a) represents a unique data set. It is one of the most frequently occupied continent-to-continent oceanographic transects in the world, with 18 occupations since 1993. There have been only two Antarctic summer seasons (1995/1996 and 1998/1999) in which the SR1b transect could not be conducted due to logistical constraints.

During the 2008/2009 season, there were two occupations of the section within 3 months, the common November-December occupation, and another in February 2009 (Table 1).

The Drake Passage hydrographic programme is a joint effort between the National Oceanography Centre in Southampton and the British Antarctic Survey in Cambridge, U.K. Most section occupations were conducted using the RRS *James Clark Ross*. Each occupation typically consists of 30 full-depth conductivity-temperature-depth (CTD) stations between Burdwood Bank and Elephant Island in the eastern Drake Passage, with a typical horizontal resolution of 30 nautical miles. In early cruises, the data were collected using a Neil Brown Instrument MkIIIc CTD, whereas the later cruises were undertaken using a SeaBird 911 plus CTD. A description of the CTD calibration and measurement errors is given in the Appendix. Characteristic distributions of potential temperature and salinity are shown in Fig. 2b,c. AABW, defined for this work as the water denser than $\gamma_n = 28.26$ kg m^{-3}, fills the abyssal layer of the southern end of the section, its northward extent being delineated by the Polar Front (Fig. 2).

In the ACC, averaging properties over a fixed latitudinal band and pressure range can introduce biases due to isopycnal heave and frontal displacement. On the other hand, the contrary, the use of neutral density (γ^n; Jackett and McDougall (1997)) as a vertical axis isolates property changes on isopycnals from those associated with heave, whilst dynamic height (ϕ) as a horizontal axis provides an accurate proxy for the cross-stream positioning of observations within the ACC. The along-section gradient in ϕ has been shown to agree well with the thermohaline definition of the ACC fronts given in Orsi et al. (1995) (see Naveira Garabato et al. (2009) for more details). Therefore, to prevent ACC frontal meandering and isopycnal heave from affecting our record of AABW properties, the data from each of the 18 repeat sections are here gridded in γ^n - ϕ space. For this study, we use ϕ at 400 dbar relative to 2000 dbar (Figure 2a) so as to exclude the influence of high-frequency upper-ocean water mass variability and of changes in the bottom layer under scrutiny here. An assessment of the propagation of the CTD measurement errors through the gridding

procedure is given in the Appendix.

b. Sea ice concentration

Monthly means of sea ice concentration from the Nimbus-7 SMMR and DMSP SSM/I-SSMIS Passive Microwave sea ice concentration measurements between October 1978 and December 2010 (Cavalieri et al. 1996) were obtained from the National Snow and Ice Data Center in Boulder, USA (http://nsidc.org/). Since 1 January 2011, the daily mean sea ice concentration based solely on DMSP SSM/I-SSMIS data (Maslanik 1999) were obtained from the same data centre, and the monthly means calculated subsequently.

3. Freshening of AABW

The SR1b repeat hydrographic section is optimally located to study changes in the AABW outflow from the Weddell Sea. It lies directly downstream of the Orkney Passage, the main gap in the South Scotia Ridge through which AABW flows into the Scotia Sea (Naveira Garabato et al. 2002b; Nowlin Jr and Zenk 1988), and a sufficient distance downstream of the AABW source regions for the substantial seasonal signal in outflow speed and properties (Gordon et al. 2010) to be largely eroded. AABW is always present at the southern end of the section, typically occupying the bottom 500-1000m of the water column south of the Polar Front (Fig. 2).

The deep Θ-S properties, gridded in dynamic height and neutral density, south of the Polar Front are shown in Figure 3. For clarity, the mean Θ-S profile for each section is shown. The two deep water masses exhibit different types of variability. The Lower Circumpolar Deep Water (LCDW), characterized by a temperature and salinity maximum, does not exhibit a long-term change in its thermohaline properties as the most recent sections (light colors) are superimposed on top of the earliest sections (Fig. 3, left panel). On the contrary, the AABW has experienced a steady decrease in salinity (and a simultaneous temperature

decrease along isopycnals) since occupation of the section commenced, as manifested in the progressive displacement of the entire deep Θ - salinity profile below 28.26 kg m^{-3} toward lower salinity values (Fig. 3, right panel).

For each section occupation, the salinity is averaged between $\gamma^n = 28.26$ kg m^{-3} (the upper bound of AABW in Drake Passage) and $\gamma^n = 28.31$ kg m^{-3} (the densest AABW class that is present in all section occupations), and the thickness of the layer bounded by the two density surfaces is calculated. This procedure excludes the component of interannual variability in AABW properties introduced by the intermittent presence of denser AABW classes, which has been shown to reflect wind-driven changes in the flow of AABW over the South Scotia Ridge (Fig. 1) rather than perturbations to AABW properties at formation (Jullion et al. 2010; Meredith et al. 2011).

The resulting time series (Fig. 4a) shows a statistically significant (at the 99% level of confidence) freshening tendency of 0.004 decade^{-1}, totalling 0.007 (std = 0.0033) between 1993 and 2011. A 2 point regression model did not find any statistically significant point of inflection in the trend, suggesting that it is not possible to determine precisely the starting time of the trend based on the available data. All the data used were collected during the same Antarctic late spring / summer season, thus reducing the possibility of any seasonal aliasing of the trend. Moreover, the two occupations in the 2008/2009 season exhibit little difference in the AABW salinity despite having been conducted three months apart (Fig. 4a), suggesting negligible intra-seasonal variability in the AABW properties. No systematic change is observed in the thickness of the AABW layer examined (Fig. 4b), indicating that there is no evidence here for a significant alteration in the rate of AABW export from the Weddell gyre.

The same analysis was done for the LCDW salinity maximum ($\gamma_n = 28.00 - 28.11$ kg m^{-3} - Fig. 4c,d) in order to investigate any inter-cruise biases. The calculated freshening trend is not statistically significant at the 90% significance level (p = 0.14). The LCDW time series is dominated by a multi annual fluctuation, with a period of no salinity change between

1993 and 2002 followed by an abrupt salinity decrease between 2003 and 2007 and a recovery between 2008 and 2012. The inter annual variability of LCDW, large compared to the AABW time series, is consistent with Provost et al. (2011) who observed large (0.01 in salinity) high frequency (3 weeks) along stream changes in the LCDW density range during two occupations of a section across Drake Passage. Moreover, there is no statistically significant correlation between the two time series (r = 0.36, p=0.13) confirming that the AABW trend is not dominated by inter-cruises biases. The magnitude of the AABW trend (0.007 between 1993 and 2012) is larger than the uncertainties associated with the propagation of measurement errors through the gridding procedure ($O(0.0005)$, see error bars on Figure 4 and Appendix for details). Overall, the absence of correlation between the AABW and LCDW salinity time series and the small errors compared with the trend suggest that the trend observed is not contaminated by inter-cruise biases or by measurement errors.

This freshening trend is approximately a factor of 2 smaller than the equivalent freshening trends reported for AABW in the Indo-Pacific sector (Jacobs and Giulivi 2010; Aoki et al. 2005; Rintoul 2007). The extent to which the factor-of-two difference in the rate of freshening is influenced by proximity to the source region (which was substantially less in the studies concerned with Indo-Pacific AABW) is unknown, though it is worth noting that intense diapycnal mixing processes in the Orkney Passage and the Scotia Sea (Naveira Garabato et al. 2004) are likely to dampen any signals of source water mass change emanating from the Weddell Sea.

The freshening of the AABW in Drake Passage may be conceivably caused by several processes. First, a change in the balance of the rates of AABW export through the different deep passages in the South Scotia Ridge, where thermohaline characteristics differ on isopycnals (Naveira Garabato et al. 2002a), could result in modified AABW properties north of the ridge. In the absence of sustained observations across all the passages, assessing variations in export routes is difficult. Nonetheless, the analysis of a recent repeat of a section of hydrographic and velocity measurements along the South Scotia Ridge in 2010 (Jullion et

al, in prep) shows no evidence of significant change relative to a section occupation in 1999 (Naveira Garabato et al. 2002b). Perturbations in wind forcing are also thought to influence the export of AABW over the Scotia Ridge (Jullion et al. 2010) on interannual and longer time scales. A decadal-scale weakening of the wind stress over the northern Weddell Sea could potentially explain the freshening by allowing colder, fresher AABW to flow through the Orkney Passage (Meredith et al. 2008). However, the decrease in wind stress that would be required for this is not supported by observations (Marshall et al. 2004). Further, such a decrease in the wind stress would also result in a reduction in the temperature and speed of the AABW outflow (Meredith et al. 2011), thereby leading to a decrease in the volume of AABW in the Scotia Sea for which there is no evidence in our observations (Fig. 4a).

Second, a change in the relative contributions of the different source waters that mix to form AABW could be responsible for the observed freshening. AABW is formed as a mixture of two main precursor water masses: the WDW (S$\sim$ 34.5, $\Theta \sim -0.5$°C) imported to the Weddell gyre from the ACC, and the high-salinity shelf waters formed during brine rejection (S$\sim$ 34.7, $\Theta \sim -1.9$°C). Any modification in the proportion in which these two primary component water masses mix could result in changes in the properties of AABW. Tracer-based studies suggest that the AABW in the northern Weddell Sea is made up of $\sim 25\%$ of shelf water. A 5% change in the source water mixing ratio would thus be enough to account for the measured freshening. However, such an increase in the proportion of WDW contributing to AABW production would also drive a warming of the AABW (by ~ 0.07°C), which is not consistent with our observations. We conclude therefore that a change in the mixing ratio of AABW source waters does not provide a plausible explanation for the observed freshening. Such a change would result in a translation along the existing Θ-S relationship, rather than the measured shift to a different Θ-S profile with lower salinities observed here.

Finally, a source water mass property change could give rise to the freshening of AABW in Drake Passage. Extensive observations of WDW and the overlying Winter Water in the

Weddell Gyre have yielded no indication of a freshening of those water masses over the period of interest (Fahrbach et al. 2011; Behrendt et al. 2011). Therefore, we deduce that the AABW freshening reported here is likely to originate from the second major precursor water mass: the dense shelf waters formed on the continental shelves of the southern or western Weddell Sea.

According to the existing literature, the AABW overflowing the South Scotia Ridge is mostly ventilated by relatively fresh shelf waters from the northeastern margin of the Antarctic Peninsula (Gordon et al. 2001), specifically from the continental shelf area off the LIS (Fahrbach et al. 1995; Huhn et al. 2008). That the vicinity of LIS is key to the formation of the AABW of interest here is also indicated by the correlation between winter sea ice concentration and AABW salinity in Drake Passage (Fig.5). The correlation is significant, reflecting the role of sea ice production in raising the salinity of the shelf waters sufficiently for them to participate in AABW formation. The lag at peak correlation (15-18 months) is consistent with an estimated transit time from the Orkney Passage to the SR1b section area of about 5 months (Meredith et al. 2011), and with an estimated transit time from the LIS region to the Orkney Passage of about 7 months (assuming a distance of 1800 km between the sill of the Orkney Passage and the tip of the Antarctic Peninsula, and a mean deep boundary current speed of 10 cm s^{-1}(Gordon et al. 2010)). The modest level of significance of the correlation ($\sim$ 80%) may be explained by a variety of factors, most notably the unavoidable simplicity of the assumed local linear relationship between sea ice concentration (the measured parameter) and production (the variable of relevance to shelf water salinity) and the relatively low number of degrees of freedom in our time series of measurements. The freshening tendency in Drake Passage is not observed within the AABW formed further south near the Filchner-Ronne Ice Shelf (Fahrbach et al. 2011), which indicates that the freshening originates downstream (to the north) of that region.

A further indication that a change in shelf water properties may be the main driver of the measured AABW freshening stems from the recent observation of a significant freshening of

the shelf waters (~ 0.09) in the western Weddell Sea between 1989 and 2006 by Hellmer et al. (2011), although we caution that this result was based on observations from only three years in that period. Since the AABW in the Weddell gyre contains around one quarter shelf waters (Meredith et al. 2000), the observed AABW freshening of ~ 0.007 requires the shelf waters off the LIS to have freshened by $\Delta S \sim -0.03$, broadly in line with the previous measurement of a shelf water freshening in the area (Hellmer et al. 2011). In the following, we seek to determine the causes of the shelf water freshening off the LIS.

4. Discussion

a. A freshwater budget of the LIS region

We construct a simplified freshwater budget of the continental shelf region off the LIS to estimate the additional (relative to the pre-freshening era) freshwater volume, V_{fw}, that is required to have entered the area to explain the observed AABW freshening. It is worth noting that any attempt to calculate an accurate estimate of V_{fw} and to precisely determine the driving mechanism are subject to significant uncertainty, given the sparse data available in the region. Therefore, we restrict our analyses to order-of-magnitude calculations, so as to identify the processes most likely to play a primary role in the freshening of the AABW.

Salt and mass conservation respectively dictate that

$$S_0 V_0 \rho_0 = S_f V_f \rho_f, \quad (1)$$

$$V_f \rho_f = V_0 \rho_0 + V_{fw} \rho_{fw}, \quad (2)$$

where ρ_0, S_0 and V_0 are the initial *in situ* density, salinity and volume of the shelf waters, and ρ_f and S_f are the *in situ* density and salinity of the shelf waters after modification by the input of an additional freshwater volume, V_{fw}, of density ρ_{fw}. Combining these two

equations, we obtain

$$V_{fw} = \frac{-V_0\rho_0}{S_f\rho_{fw}}(S_f - S_0). \quad (3)$$

We set $\rho_0 = 1027$ kg m^{-3} and $\rho_{fw} = 1000$ kg m^{-3}. We define V_0 as the volume of the continental shelf adjacent to the LIS where shelf water salinity has been observed to exceed the threshold value for AABW ventilation (Gill 1973). Using available *in situ* data on the continental shelf (Fig. 1b), the latitudinal extent of the shelf area where the bottom salinity of the shelf waters was greater than Gill's (1973) threshold is approximated ($64^\circ - 70^\circ$S). The longitudinal extent of the control volume is defined by the coast and the 1000m isobath based on the GEBCO One Minute bathymetry (http://www.gebco.net/), and the average depth of the shelf is estimated to be approximately 500 m. This yields $V_0 \sim 9.10^{13}$ m^3. To estimate S_f, we refer to the most recent stations in the control area, occupied in 2004 (Fig. 1b), which reveal that $S_f \sim 34.6$. Thus, we find that $V_{fw} \approx 8 \times 10^{10}$ m^3.

b. Origin of the freshening

This excess freshwater supply to the control area may have been associated with three mechanisms: an increase in net precipitation; a reduction in sea ice production; or an increase in freshwater runoff from the LIS and tributary glaciers. The plausibility of each of these mechanisms contributing significantly to the observed shelf water freshening is examined next.

1) Precipitation

In order for the excess freshwater V_{fw} to have been supplied by an increase in net precipitation in the continental shelf region off the LIS, an additional ~ 40 cm of freshwater is required to have precipitated there between 1993 and 2011, relative to the pre-freshening era. Estimates of net precipitation in the oceanic region adjacent to the LIS are on the order of 50 cm yr^{-1} (Bromwich et al. 2011; Munneke et al. 2012), so that a modest percentage

increase in the annual-mean value would have been sufficient to account for the observed freshening signal. A recent intercomparison of several atmospheric reanalyses revealed no detectable decadal-scale tendency in net precipitation in our control region (Bromwich et al. 2011). Thus, whilst the uncertainties in the reanalyses do not allow us to rule it out, the scenario of a major contribution to V_{fw} from an increase in net precipitation is not supported by an existing evidence.

2) Sea ice

Sea ice production in winter is a key process in the formation of AABW, as the resulting brine rejection makes shelf waters dense enough to cascade down the continental slope. Thus, sea ice production acts as the main transmitter of any climatic signal imprinted in shelf waters (regardless of the signal's origin) to the AABW layer, and one can expect a relationship between variability in sea ice concentration near the LIS and AABW salinity in Drake Passage. The existence of such a relationship is suggested by the substantial degree of positive correlation that occurs between interannual-scale fluctuations in AABW salinity in the SR1b section and sea ice concentration anomalies off the LIS (Fig.5a). The pattern of the correlation and its lag (15-18 months), described in the previous section, suggest that a reduction in sea ice production cannot be excluded as a contributor to the observed AABW freshening trend.

The plausibility of this contribution may be assessed by considering, once again, a simple freshwater budget. Salt and mass conservation dictate that

$$\rho_0 V_0 S_0 = \rho_f V_f S_f + \rho_{si} V_{si} S_{si}, \tag{4}$$

$$\rho_0 V_0 = \rho_f V_f + \rho_{si} V_{si}, \tag{5}$$

where $\rho_{si} = 920$ kg m^{-3} and $S_{si} = 6$ are the characteristic density and salinity of sea ice, respectively (Eicken 1997), and V_{si} is a change in sea ice volume. From these expressions, we estimate the reduction in sea ice production required to explain the observed freshening

as

$$V_{si} = -\frac{\rho_0 V_0}{\rho_{si}(S_f - S_{si})}(S_f - S_0), \quad (6)$$

and obtain $V_{si} \approx 1.1 \times 10^{11}$ m^3 by substituting the appropriate values quoted above. Assuming a full sea ice cover over the control area ($\sim 2 \times 10^{11}$ m^2) in winter (Stammerjohn et al. 2008) and a characteristic sea ice thickness of 2 m (Zwally et al. 2008), this value of V_{si} implies that a reduction of $\sim 25\%$ of the total sea ice production between 1993 and 2011 (or a $\sim 1\%$ decrease in the net annual sea ice production averaged between 1993 and 2011) is required to account for the observed freshening signal. In the absence of reliable estimates of sea ice production near the LIS, assessing the extent to which a reduction in sea ice production may explain the observed AABW freshening is difficult. Tamura et al. (2008) used sea ice concentration data from satellite and air-sea reanalysis products to estimate the sea ice production in several polynyas around Antarctica (but not near the LIS) and reported a 30% decrease in the production of sea ice in Weddell Sea polynyas between 1992 and 2001. Whilst this result suggests that trends of the correct sign and order of magnitude are at least plausible in the region, the lack of appropriate sea ice production estimates for the LIS area prevents us from making a definitive statement on the importance of reduced sea ice production in the observed AABW freshening.

3) Increased glacial loss

The glaciers and ice shelves of the eastern Antarctic Peninsula have undergone considerable changes over the last 15 years. The break up of major ice shelves (Larsen A in 1995 (Rott et al. 1996) and Larsen B in 2002, (Scambos et al. 2003)) and the subsequent acceleration of their tributary glaciers due to the removal of the ice shelves' buttressing effect (Rignot et al. 2004; Shuman et al. 2011) has resulted in a large volume of ice being discharged to the ocean in the control area of our freshwater budget. We estimate the net excess freshwater loss by

the ice shelves and their tributary glaciers by collating the findings of a range of glaciological studies (Table 2), and conclude that the volume of freshwater added to the continental shelf off the LIS between 1993 and 2011 was $V_{gi} \sim 3.2 \times 10^{12}$ m^3. The bulk of V_{gi} ($\sim 3 \times 10^{12}$ m^3) is contributed by the disintegration of the ice shelves themselves, whereas the contribution of accelerated tributary glaciers is an order of magnitude smaller ($\sim 2 \times 10^{11}$ m^3).

Whilst V_{gi} dwarfs our estimate of the volume of excess freshwater required to explain the observed freshening signal by two orders of magnitude, the fraction of V_{gi} that enters the continental shelf in liquid form and thereby effects a freshening of the local shelf waters is uncertain, as it depends on the poorly constrained trajectories and melt rates of the numerous small icebergs into which the Larsen A and B ice shelves fragmented (Scambos et al. 2003; MacAyeal et al. 2003). In the western Weddell Sea, icebergs have been observed to drift at rates on the order of 400 m h^{-1} (Rack and Rott 2004; Schodlok et al. 2006). The area loss during the collapse of the Larsen A and B ice shelves has been estimated to be around 1.1×10^{10} m^2 (Rack and Rott 2004). Given the characteristic iceberg drift rate and the width of the continental shelf in front of the LIS (∼300 km), the residence time of the icebergs generated by the Larsen A and B ice shelf disintegration events may be crudely estimated at around 1 month. The melting rates of icebergs are uncertain and depend upon iceberg size, geometry and adjacent meteorological (air temperature) and oceanographic (water temperature) conditions. Observed and modelled melt rates vary by one order of magnitude (0.2-2 m month^{-1} Schodlok et al. (2006); Jansen et al. (2007)). Taking these rates to be representative, the volume lost on the continental shelf off the LIS by the icebergs resulting from the ice shelf collapses may then be estimated as $0.2 - 2 \times 10^{10}$ m^3, which is substantially less than V_{fw}. Whilst the uncertainty surrounding several steps of this calculation again prevents us from being categorical, the estimate suggests that the icebergs deriving from the disintegration of the A and B sectors of the LIS probably played a temporary or minor role in freshening the local shelf waters.

The mass loss resulting from the Larsen A and B tributary glaciers after the ice shelf break

ups is likely to provide a more significant and persistent source of freshwater to the coastal region off the LIS over the study period than the disintegration of the ice shelves themselves. Silva et al. (2006) reported a modelled total iceberg melt rate of 0.5 m m^{-2} y^{-1} for the western Weddell Sea and showed that only 3 % of small icebergs (such as those generated by the acceleration of LIS tributary glaciers) reach north of 63°S, suggesting a significant melting of small icebergs in the coastal region to the east of the Antarctic Peninsula. Since the accelerated LIS thinning and retreat rate is still one order of magnitude larger than V_{fw} ($\sim 2 \times 10^{11}$ m^3; Table 2), a melting of only 25% of the resulting small icebergs within the LIS region would be sufficient to explain the observed AABW freshening. This scenario appears plausible in light of the preceding argument, leading us to conclude that increased glacial loss from the LIS is likely to be a significant player in the freshening.

5. Conclusion

A time series of AABW salinity in Drake Passage has been constructed using 18 repeats of the SR1b hydrographic section between 1993 and 2010. A significant freshening of the bottom water (0.004 $decade^{-1}$) has been reported with no significant decrease in the thickness of the AABW layer. We deduce that increased glacial loss from the Antarctic Peninsula following the break up of the Larsen A and B ice shelves is likely to have contributed significantly to the observed AABW freshening. The implication of reduced sea ice production or increased precipitation off the LIS in the freshening cannot be ruled out with the available data, but the sheer size of the glacial contribution suggests that it may be the dominant driver.

There is evidence that the AABW freshening in the Indo-Pacific sector of the Southern Ocean is primarily forced by deglaciation in areas of West Antarctica, where an ocean-induced enhancement of basal melting has been observed in recent decades (Jacobs et al. 2002; Rintoul 2007; Jacobs and Giulivi 2010; Pritchard et al. 2012). In contrast, the changes in glacial runoff in the western Weddell Sea that primarily underpin the freshening of the

region's AABW outflow are argued here to result from atmospheric forcing. The collapse of the Larsen A and B ice shelves and the subsequent acceleration in glacial runoff have been linked to the summertime intensification of the circumpolar westerly winds over the Southern Ocean in recent decades (Scambos et al. 2003; van den Broeke 2005), which has been attributed in part to anthropogenic processes including ozone depletion (Thompson and Solomon 2002). The intensification of the westerlies has been shown to lead to a weakening of the blocking effect of the Antarctic Peninsula orography, with the associated promotion of advection of relatively warm maritime air onto the eastern side of the Peninsula (Orr et al. 2004; Marshall et al. 2006) raising regional summer temperatures by 2°C over the last four decades (King et al. 2004). This summer warming has been highlighted as pivotal in the enhanced surface melting of the LIS that heralded the collapse of large sectors of the ice shelf around the turn of the century (Scambos et al. 2003; van den Broeke 2005). Consequently, to the extent that the AABW freshening observed here can be attributed to the collapse of parts of the LIS and acceleration of its tributary glaciers, the same freshening can also be attributed to the strengthening atmospheric circulation over this part of the Southern Ocean, with a previously argued anthropogenic cause.

A continuation of the AABW freshening tendency over the coming decades may be expected on the basis of our present glaciological knowledge of the LIS region. For example, the acceleration of glacial runoff in the Larsen B area observed over the last 15 years is expected to persist into the years to come (Shuman et al. 2011). Further, the intact Larsen C Ice Shelf contains a volume of freshwater that is greater than that in the collapsed Larsen A and B sectors by an order of magnitude, and buttresses a much larger glacial catchment. Larsen C is already thinning in response to variations in climatic forcing (Shepherd et al. 2003; Fricker and Padman 2012), and its snow-pack is showing signs of meltwater influence (Holland et al. 2011). These changes seemingly herald a progression towards the point at which further atmospheric melting may drive crevassing and ice-shelf failure, following which a large volume of freshwater is expected to enter the continental shelf region off the LIS from

which the AABW outflow from the Weddell Sea is ventilated.

The freshening of Atlantic-sourced AABW reported here completes a circumpolar-wide pattern of AABW freshening, albeit with different mechanisms being important in different sectors. As much of the AABW exported through the Orkney Passage ultimately escapes the Scotia Sea into the wider South Atlantic (Naveira Garabato et al. 2002a), our results suggest that the AABW feeding the lower limb of the Atlantic Overturning Circulation is freshening. Relating this freshening to the strength of the lower limb of the Atlantic MOC is not straightforward: it is possible that horizontal density gradients may be modified, with impacts on abyssal current speeds. However, the broad-scale finding of an AABW freshening in Drake Passage with no attendant decrease in layer thickness argues that the formation rate has not changed discernibly, and that it is formation properties that are being climatically altered. We have argued that dense water production in the Weddell Sea is sensitive to the impact of regional and large-scale decadal climatic change, and that the Weddell gyre does not insulate the bottom water formation regions from such change.

Acknowledgments.

We thank the National Environmental Research Council for financial support of the Antarctic Deep Rates of Export project (NE/E01366X/1). The SR1b section is a joint effort between the National Oceanography Centre, Southampton (NOCS) and the British Antarctic Survey (BAS) in Cambridge, U.K. Researchers and students from other institutions have also made invaluable contributions to the cruises. The measurements could not have been achieved without the willing cooperation and support of the planning and operations groups at NOCS and BAS. We are grateful to two anonymous reviewers for useful comments, which contributed to improving the quality of the paper. Finally, we gratefully acknowledge the outstanding contribution of the Masters, officers and crew of RRS *James Clark Ross* and RRS *James Cook*.

APPENDIX

CTD calibration, data accuracy and errors

To detect water mass changes in the deep ocean, it is necessary to quantitatively assess the data quality, as the signals of change are small and can potentially be affected by measurement error and inter-cruise biases. Here we investigate CTD measurement errors and the propagation of these errors through the procedure of gridding in density and dynamic height coordinates. Salinity errors are particulary important here, because the reported signal is a freshening, and because salinity is the dominant factor in density changes at low temperature.

a. CTD measurement error

We conduct an error analysis similar to that of Naveira Garabato et al. (2009) and Williams et al. (2006) who used the same data set to investigate the variability of other water masses. Starting with the measurement error, we define the error on the CTD data as the quadratic sum of 2 terms:

$$\sigma_{ctd} = \sqrt{\sigma_{sy}^2 + \sigma_{sb}^2} \tag{A1}$$

where σ_{sy}^2 is the systematic error representing the accuracy of the measurement of a tracer and σ_{sb} is the sampling error both in the vertical and the horizontal directions. Sampling error is particularly important for bottle data because of their coarse vertical resolution. CTD data have a much higher vertical resolution (1 or 2 dbar when averaged) but still suffer from a limited horizontal resolution (the station spacing) and might be affected by small scale structures. The sampling error is estimated by horizontally subsampling the 1997 section

(which had 50 stations instead of the usual 32) and regridding the subsampled section to calculate the mean salinity and temperature of the AABW. The sampling error is found to be 0.002 in salinity and 0.002°C in temperature.

The systematic error represents the accuracy of the measurement of a tracer. A detailed account of the data processing can be found in the individual cruise reports (`http://www.noc.soton.ac.uk/ooc/TRANSPORTS/DrakePassage.php`). For each cruise, the CTD data were carefully analyzed in order to identify and correct for potential issues with the data. Concerning the pressure and temperature measurements, cruise reports show that the data accuracy is $\sigma_{ctdT} = 1$ db in pressure and $\sigma_{ctdT} = 1 \times 10^{-3}$ °C in temperature.

CTD conductivity sensors, particularly in the early cruises, were subject to drift and imprecisions in the measurements, requiring that the CTD data are calibrated against conductivity measured in water samples collected at different depths during station occupations. Twelve water samples covering the whole water column were typically taken at each station. Conductivity/salinity was measured for each water sample using a Guildline Autosal 8400B salinometer. The salinometer was standardized using IAPSO Standard Seawater - SSW (Table 1 for details on the different batch used). The differences between the CTD salinity and bottle data were calculated and, if necessary, offsets were applied to minimize the residuals between the CTD and bottle conductivites (In 94/95, due to issue with the conductivity cell, extra care was taken and the CTD-bottle differences were examined on a station by station basis so that the mean difference between the bottle and CTD salinities is -1×10^{-4}). Several duplicates were taken during each cruise to monitor the performance of the salinometer and the differences between duplicates were found to be of the order 1×10^{-4}.Furthermore, the quality of the CTD salinity increased with improvements in the CTD sensors and few/small corrections were needed in the most recent cruises.

The accuracy and reliability of the SSW has been investigated by several independent groups (Mantyla 1980, 1987, 1994; Kawano et al. 2006; Bacon et al. 2000, 2007). The accuracy and consistency of the different batch of SSW is important as they are used to

calibrate the salinometer and thus help calibrate both the bottle and CTD salinity. Kawano et al. (2006), found that the batch to batch differences improved significantly since the 1980s and the standard deviation of is 0.3×10^{-3}. Their proposed correction for the SSW batch used during the different SR1b cruises is of the order 1×10^{-3}. Moreover, Bacon et al. (2007) performed a detailed analysis of the uncertainties and stability of the SSW manufacturing process. They demonstrated that there was no significant change in the label conductivity ratio for SSW batches P130 to P144 outside the uncertainty of the conductivity ratio. Gouretski and Jancke (2000) analyzed a large hydrographic data set and found that difference in SSW batch did not seem to be the main cause of inter-cruise biases. The systematic error resulting from the CTD calibration and SSW batch differences is therefore small (2×10^{-3}).

b. Error propagation

These errors on the CTD salinity data propagate through our salinity field gridded in $\gamma_n - \Phi$ 1) by affecting the values of salinity used to calculate the mean and 2) by biasing the coordinate system as both density and dynamic height are a function of salinity. Errors in temperature and pressure measurement also impact on the calculation of density and dynamic height. Isolating the relative contribution of the two on the mean salinity of the AABW is difficult and instead we investigate their combined effect. To estimate the influence of these errors, we introduce in each temperature, salinity and pressure field an error:

$$S = S + \sigma_{ctdS}$$

$$T = T + \sigma_{ctdT}$$

$$P = P + \sigma_{ctdP}$$

where σ_{ctdS}, σ_{ctdT} and σ_{ctdP} are normally-distributed random errors with mean equal to zero and standard deviation equal to 2.8×10^{-3}, 2.2×10^{-3}°C and 1 db respectively. The

same gridding procedure is then applied using the biased fields and the mean AABW salinity and thickness are then calculated and compared with our time series. The mean regridding errors calculated are $\sigma_{rgS} = 6 \times 10^{-4}$ (std $= 6 \times 10^{-4}$) and $\sigma_{rgTh} = 30.7m$ (std 37.5 m) for the mean AABW salinity and thickness respectively.

The final error to consider is the standard error of the mean salinity, σ_{se}, defined as:

$$\sigma_e = \frac{s}{\sqrt{n}} \tag{A2}$$

where s is the standard deviation of the salinity mean for a given cruise and n is the number of samples (the number of grid points used to calculate the mean). The mean standard error found here is $\sigma_{eS} = 4 \times 10^{-4}$ for salinity and $\sigma_{eTh} = 32.4$ m for the thickness.

The total error on salinity is $\sigma_S = \sqrt{\sigma_{eS}^2 + \sigma_{rgS}^2}$ and on thickness is $\sigma_{Th} = \sqrt{\sigma_{eTh}^2 + \sigma_{rgTh}^2}$. The errors are plotted as error bar on Figure 4. The error analysis reveals that the observed salinity trend is larger than the potential errors coming from CTD measurement errors and their subsequent propagation through the derived quantities presented in this study.

REFERENCES

Aoki, S., S. Rintoul, S. Ushio, S. Watanabe, and N. Bindoff, 2005: Freshening of the adelie land bottom water near 140 degrees e. *Geophys. Res Letters*, **32 (23)**, L23 601, doi:10.1029/2005GL024246.

Bacon, S., F. Culkin, N. Higgs, and P. Ridout, 2007: Iapso standard seawater: Definition of the uncertainty in the calibration procedure, and stability of recent batches. *J. Atm. Oceanic Technol.*, **24**, 1785–1799.

Bacon, S., H. Snaith, and M. Yelland, 2000: An evaluation of some recent batches of iapso standard seawater. *J. Atm. Oceanic Technol.*, **17**, 854–861.

Behrendt, A., E. Fahrbach, M. Hoppema, G. Rohardt, O. Boebel, O. Klatt, A. Wisotzki, and H. Witte, 2011: Variations of winter water properties and sea ice along the greenwich meridian on decadal time scales. *Deep-Sea Research II*, **58 (25-26)**, 2524–2532, doi:10.1016/j.dsr2.2011.07.001.

Berthier, E., T. A. Scambos, and C. A. Shuman, 2012: Mass loss of larsen b tributary glaciers (antarctic peninsula) unabated since 2002. *Geophysical Research Letters*, **39 (13)**, L13 501, doi:10.1029/2012GL051755.

Bromwich, D. H., J. P. Nicolas, and A. J. Monaghan, 2011: An assessment of precipitation changes over antarctica and the southern ocean since 1989 in contemporary global reanalyses. *J. Climate*, **24 (16)**, 4189–4209, doi:10.1175/2011JCLI4074.1.

Carmack, E. and T. Foster, 1975: Flow of water out of the weddell sea. *Deep-Sea Research*, **22 (11)**, 711–724.

Cavalieri, D., C. Parkinson, P. Gloersen, and H. J. Zwally, 1996: Sea ice concentrations from nimbus-7 smmr and dmsp ssm/i-ssmis passive microwave data. Tech. rep., National Snow and Ice Data Center,Boulder, Colorado, USA.

Church, J. A., et al., 2011: Revisiting the earth's sea-level and energy budgets from 1961 to 2008. *Geophys. Res Letters*, **38 (18)**, L18 601, doi:10.1029/2011GL048794.

Eicken, H., 1997: Salinity profiles of antarctic sea ice: Field data and model results. *J. Geophys. Res.-Oceans*, **97 (C10)**, 15,545–15,557, doi:10.1029/92JC01588.

Fahrbach, E., M. Hoppema, G. Rohardt, O. Boebel, O. Klatt, and A. Wisotzki, 2011: Warming of deep and abyssal water masses along the greenwich meridian on decadal time scales the weddell gyre as a heat buffer. *Deep-Sea Research II*, **58 (25-26)**, 2509–2523, doi:10.1016/j.dsr2.2011.06.007.

Fahrbach, E., G. Rohardt, N. Scheele, M. Schröder, V. Strass, and A. Wisotzki, 1995: Formation and discharge of deep and bottom water in the northwestern Weddell Sea. *J. Mar. Res.*, **53 (4)**, 515–538.

Foldvik, A., et al., 2004: Ice shelf water overflow and bottom water formation in the southern weddell sea. *J. Geophys. Res.*, **109**, C02 015.

Foster, T. and E. Carmack, 1976: Frontal zone mixing and antarctic bottom water formation in the southern weddell sea. *Deep-Sea Research*, **23 (4)**, 301–317.

Fricker, H. A. and L. Padman, 2012: Thirty years of elevation change on antarctic peninsula ice shelves from multimission satellite radar altimetry. *J. Geophys. Res.-Oceans*, **117**, C02 026, doi:10.1029/2011JC007126.

Gill, A., 1973: Circulation and bottom water production in the weddell sea. *Deep-Sea Research*, **20 (2)**, 111–140.

Gordon, A. L., B. Huber, D. Mckee, and M. Visbeck, 2010: A seasonal cycle in the export of bottom water from the weddell sea. *Nature Geoscience*, **3 (8)**, 551–556, doi:10.1038/ngeo916.

Gordon, A. L., M. Visbeck, and B. Huber, 2001: Export of Weddell Sea Deep and Bottom Water. *J. Geophys. Res.-Oceans*, **106 (C5)**, 9005–9017.

Gouretski, V. and K. Jancke, 2000: Systematic errors as the cause for an apparent deep water property variability: global analysis of the woce and historical hydrographic data. *Prog. Oceanogr.*, **48 (4)**, 337–402.

Hellmer, H. H., O. Huhn, D. Gomis, and R. Timmermann, 2011: On the freshening of the northwestern weddell sea continental shelf. *Oc. Sc.*, **7 (3)**, 305–316, doi:10.5194/os-7-305-2011.

Hellmer, H. H., F. Kauker, R. Timmermann, J. Determann, and J. Rae, 2012: Twenty-first-century warming of a large antarctic ice-shelf cavity by a redirected coastal current. *Nature*, **485 (7397)**, 225–228, doi:10.1038/nature11064.

Holland, P. R., H. F. J. Corr, H. D. Pritchard, D. G. Vaughan, R. J. Arthern, A. Jenkins, and M. Tedesco, 2011: The air content of larsen ice shelf. *Geophys. Res Letters*, **38 (10)**, L10 503, doi:10.1029/2011GL047245.

Huhn, O., H. H. Hellmer, M. Rhein, C. Rodehacke, W. Roether, M. Schodlok, and M. Schroder, 2008: Evidence of deep-and bottom-water formation in the western weddell sea. *Deep-Sea Research II*, **55 (8-9)**, 1098–1116.

Jackett, D. and T. McDougall, 1997: A neutral density variable for the world's oceans. *J. Phys. Oceanogr.*, **27 (2)**, 237–263.

Jacobs, S., C. Giulivi, and P. Mele, 2002: Freshening of the ross sea during the late 20th century. *Science*, **297 (5580)**, 386–389.

603 Jacobs, S. S., 2004: Bottom water production and its links with the thermohaline circulation.
604 *Antarctic Science*, **16 (4)**, 427–437, doi:10.1017/S095410200400224X.

605 Jacobs, S. S. and C. F. Giulivi, 2010: Large multidecadal salinity trends near the pacific–
606 antarctic continental margin. *J. Climate*, **23 (17)**, 4508–4524, doi:10.1175/2010JCLI3284.
607 1.

608 Jacobs, S. S., A. Jenkins, C. F. Giulivi, and P. Dutrieux, 2011: Stronger ocean circulation
609 and increased melting under pine island glacier ice shelf. *Nature Geoscience*, **4 (8)**, 519–
610 523, doi:10.1038/ngeo1188.

611 Jansen, D., M. Schodlok, and W. Rack, 2007: Basal melting of a-38b: a physical model
612 constrained by satellite observations. *Remote Sensing of Environment*, **111 (2)**, 195–203.

613 Johnson, G. C. and S. C. Doney, 2006: Recent western South Atlantic bottom water warm-
614 ing. *Geophys. Res Letters*, **33**, L14 614.

615 Johnson, G. C., S. G. Purkey, and J. L. Bullister, 2008a: Warming and freshening in the
616 abyssal southeastern Indian Ocean. *J. Climate*, **21 (20)**, 5351–5363.

617 Johnson, G. C., S. G. Purkey, and J. M. Toole, 2008b: Reduced Antarctic meridional over-
618 turning circulation reaches the North Atlantic Ocean. *Geophys. Res Letters*, **35 (22)**,
619 L22 601.

620 Jullion, L., S. C. Jones, A. C. N. Garabato, and M. P. Meredith, 2010: Wind-controlled
621 export of antarctic bottom water from the weddell sea. *Geophys. Res Letters*, **37 (9)**,
622 L09 609, doi:10.1029/2010GL042822.

623 Kawano, T., M. Aoyama, T. Joyce, H. Uchida, Y. Takatsuki, and M. Fukasawa, 2006: The
624 latest batch-to-batch difference table of standard seawater and its application to the woce
625 onetime sections. *J. Oceanography*, **62**, 777–792.

Killworth, P., 1974: Baroclinic model of motions on antarctic continental shelves. *Deep-Sea Research*, **21 (10)**, 815–837.

King, J., J. Turner, G. Marshall, W. Connolley, and T. Lachlan-Cope, 2004: Antarctic peninsula climate variability and its causes as revealed by analysis of instrumental records. *Antarctic Peninsula Climate Variability: A historical and Paleoenvironmental Perspective.*, E. Domack, A. Burnett, P. Convey, M. Kirby, and R. Bindschadler, Eds., American Geophysical Union, Washington D.C. USA, Vol. 79, 17–30.

MacAyeal, D., T. Scambos, C. Hulbe, and M. Fahnestock, 2003: Catastrophic ice-shelf break-up by an ice-shelf-fragment-capsize mechanism. *J. Glaciology*, **49 (164)**, 22–36.

Mantyla, A., 1980: Electric conductivity comparisons of standard seawater batches p29 to p84. *Deep-Sea Research I*, **27**, 837–846.

Mantyla, A., 1987: Standard seawater comparisons updated. *J. Phys. Oceanogr.*, **17**, 543–548.

Mantyla, A., 1994: The treatment of inconsistencies in atlantic deep water salinity data. *Deep-Sea Research*, **41**, 1387–1405.

Marshall, G. J., A. Orr, N. P. M. van Lipzig, and J. King, 2006: The impact of a changing southern hemisphere annular mode on antarctic peninsula summer temperatures. *J. Climate*, **19 (20)**, 5388–5404.

Marshall, G. J., P. A. Stott, J. Turner, W. M. Connolley, J. C. King, and T. A. Lachlan-Cope, 2004: Causes of exceptional atmospheric circulation changes in the Southern Hemisphere. *Geophys. Res Letters*, **31 (14)**, L14 205.

Maslanik, J., 1999: Near-real-time dmsp ssm/i-ssmis daily polar gridded sea ice concentrations. Tech. rep., National Snow and Ice Data Center,Boulder, Colorado, USA.

649 Meredith, M., R. Locarnini, K. V. Scoy, A. Watson, K. Heywood, and B. King, 2000: On the
650 sources of Weddell Gyre Antarctic Bottom Water. *J. Geophys. Res.-Oceans*, **105 (C1)**,
651 1093–1104.

652 Meredith, M. P., A. L. Gordon, A. C. N. Garabato, E. P. Abrahamsen, B. A. Huber, L. Jul-
653 lion, and H. J. Venables, 2011: Synchronous intensification and warming of antarctic
654 bottom water outflow from the weddell gyre. *Geophys. Res Letters*, **38 (3)**, L03 603, doi:
655 10.1029/2010GL046265.

656 Meredith, M. P., A. C. Naveira Garabato, A. L. Gordon, and G. C. Johnson, 2008: Evolution
657 of the Deep and Bottom Waters of the Scotia Sea, Southern Ocean, during 1995–2005. *J.*
658 *Climate*, **21 (13)**, 3327–3343.

659 Munneke, P. K., G. Picard, M. R. V. D. Broeke, J. T. M. Lenaerts, and E. V. Meijgaard,
660 2012: Insignificant change in antarctic snowmelt volume since 1979. *Geophys. Res Letters*,
661 **39 (1)**, L01 501, doi:10.1029/2011GL050207.

662 Naveira Garabato, A. C., K. J. Heywood, and D. P. Stevens, 2002a: Modification and
663 pathways of Southern Ocean deep waters in the Scotia Sea. *Deep-Sea Research I*, **49 (4)**,
664 681–705.

665 Naveira Garabato, A. C., L. Jullion, D. P. Stevens, K. J. Heywood, and B. A. King, 2009:
666 Variability of Subantarctic Mode Water and Antarctic Intermediate Water in the Drake
667 Passage during the Late-Twentieth and Early-Twenty-First Century. *J. Climate*, **22**, 3661–
668 3688, doi:10.1175/2009JCLI2621.1.

669 Naveira Garabato, A. C., E. McDonagh, D. P. Stevens, K. J. Heywood, and R. J. Sanders,
670 2002b: On the export of Antarctic Bottom Water from the Weddell Sea. *Deep-Sea Research*
671 *II*, **49**, 4715–4742.

672 Naveira Garabato, A. C., K. L. Polzin, B. King, K. J. Heywood, and M. Visbeck, 2004:
673 Widespread intense turbulent mixing in the Southern Ocean. *Science*, **303**, 210–213.

674 Nicholls, K. W., S. Østerhus, K. Makinson, T. Gammelsrød, and E. Fahrbach, 2009: Ice-
675 ocean processes over the continental shelf of the southern Weddell Sea, Antarctica: A
676 review. *Rev. Geophys.*, **47 (3)**, 2007RG000 250.

677 Nowlin Jr, W. and W. Zenk, 1988: Westward bottom currents along the margin of the south
678 shetland island arc. *Deep-Sea Research I*, **35 (2)**, 269–301.

679 Orr, A., D. Cresswell, G. J. Marshall, J. Hunt, J. Sommeria, C. Wang, and M. Light, 2004:
680 A 'low-level'explanation for the recent large warming trend over the western antarctic
681 peninsula involving blocked winds and changes in zonal circulation. *Geophys. Res Letters*,
682 **31 (6)**, L06 204,, doi:10.1029/2003GL019160.

683 Orsi, A., T. Whitworth, and W. D. Nowlin, 1995: On the meridional extent and fronts of
684 the Antarctic Circumpolar Current. *Deep-Sea Research I*, **42 (5)**, 641–673.

685 Orsi, A. H., G. C. Johnson, and J. L. Bullister, 1999: Circulation, mixing, and production
686 of Antarctic Bottom Water. *Prog. Oceanogr.*, **43 (1)**, 55–109.

687 Pritchard, H. D., S. R. M. Ligtenberg, H. A. Fricker, D. G. Vaughan, M. R. van den Broeke,
688 and L. Padman, 2012: Antarctic ice-sheet loss driven by basal melting of ice shelves.
689 *Nature*, **484 (7395)**, 502–505, doi:10.1038/nature10968.

690 Provost, C., A. Renault, N. Barré, N. Sennéchael, V. Garçon, J. Sudre, and O. Huhn, 2011:
691 Two repeat crossings of Drake Passage in austral summer 2006 Short-term variations and
692 evidence for considerable ventilation of intermediate and deep waters. *Deep-Sea Research*
693 *II*, **58 (25-26)**, 2555–2571.

694 Purkey, S. G. and G. C. Johnson, 2010: Warming of global abyssal and deep southern
695 ocean waters between the 1990s and 2000s: Contributions to global heat and sea level rise
696 budgets. *Journal of Climate*, **23 (23)**, 6336–6351, doi:10.1175/2010JCLI3682.1.

Purkey, S. G. and G. C. Johnson, 2012: Global contraction of antarctic bottom water between the 1980s and 2000s. *J. Climate*, **25 (17)**, 5830–5844, doi:10.1175/JCLI-D-11-00612.1.

Rack, W. and H. Rott, 2004: Pattern of retreat and disintegration of the larsen b ice shelf, antarctic peninsula. *Annals of Glaciology*, **39 (1)**, 505–510.

Rignot, E., 2006: Changes in ice dynamics and mass balance of the antarctic ice sheet. *Philos T R Soc A*, **364**, 1637–1655, doi:doi:10.1098/rsta.2006.1793.

Rignot, E., G. Casassa, P. Gogineni, W. Krabill, A. Rivera, and R. Thomas, 2004: Accelerated ice discharge from the antarctic peninsula following the collapse of larsen b ice shelf. *Geophys. Res Letters*, **31 (18)**, L18 401, doi:10.1029/2004GL020697.

Rintoul, S. R., 2007: Rapid freshening of antarctic bottom water formed in the indian and pacific oceans. *Geophys. Res Letters*, **34 (6)**, L06 606, doi:10.1029/2006GL028550.

Roemmich, D., G. Johnson, S. Riser, R. Davis, J. Gilson, W. Owens, C. Schmid, and M. Ignaszewski, 2009: The argo program: Observing the global oceans with profiling floats. *Oceanography*, **22**, 24–33.

Rott, H., F. Müller, T. Nagler, and D. Floricioiu, 2011: The imbalance of glaciers after disintegration of larsen-b ice shelf, antarctic peninsula. *The Cryosphere*, **5 (1)**, 125–134, doi:10.5194/tc-5-125-2011.

Rott, H., P. Skvarca, and T. Nagler., 1996: Rapid collapse of northern larsen ice shelf, antarctica. *Science*, **271 (5250)**, 788–792, doi:10.1126/science.271.5250.788.

Scambos, T. A., C. Hulbe, and M. Fahnestock, 2003: Climate-induced ice shelf disintegration in the antarctic peninsula. *Antarctic Research Series*, **79**, 79–92.

Schodlok, M. P., H. H. Hellmer, G. Rohardt, and E. Fahrbach, 2006: Weddell sea iceberg drift: Five years of observations. *J. Geophys. Res.*, **111 (C6)**, C06 018, doi:10.1029/2004JC002661.

721 Shepherd, A., D. Wingham, T. Payne, and P. Skvarca, 2003: Larsen ice shelf has progres-
722 sively thinned. *Science*, **302 (5646)**, 856–859.

723 Shepherd, A., D. Wingham, and E. Rignot, 2004: Warm ocean is eroding west antarctic ice
724 sheet. *Geophys. Res Letters*, **31 (23)**, L23 402, doi:10.1029/2004GL021106.

725 Shepherd, A., D. Wingham, D. Wallis, K. Giles, S. Laxon, and A. V. Sundal, 2010: Recent
726 loss of floating ice and the consequent sea level contribution. *Geophys. Res Letters*, **37 (13)**,
727 L13 503, doi:10.1029/2010GL042496.

728 Shuman, C., E. Berthier, and T. Scambos, 2011: 2001–2009 elevation and mass losses in the
729 larsen a and b embayments, antarctic peninsula. *Journal of Glaciology*.

730 Silva, T. A. M., G. R. Bigg, and K. W. Nicholls, 2006: Contribution of giant icebergs to
731 the southern ocean freshwater flux. *J. Geophys. Res.*, **111 (C3)**, C03 004, doi:10.1029/
732 2004JC002843.

733 Stammerjohn, S. E., D. G. Martinson, R. C. Smith, X. Yuan, and D. Rind, 2008: Trends
734 in antarctic annual sea ice retreat and advance and their relation to el niño–southern
735 oscillation and southern annular mode variability. *J. Geophys. Res.*, **113 (C3)**, C03S90,
736 doi:10.1029/2007JC004269.

737 Sutherland, W., et al., 2012: A horizon scan of global conservation issues for 2012. *Trends*
738 *in Ecol. and Ev.*, doi:10.1016/j.tree2011.10.011.

739 Tamura, T., K. I. Ohshima, and S. Nihashi, 2008: Mapping of sea ice production for
740 antarctic coastal polynyas. *Geophysical Research Letters*, **35 (7)**, L07 606, doi:10.1029/
741 2007GL032903.

742 Thoma, M., A. Jenkins, D. Holland, and S. Jacobs, 2008: Location and timing of Cir-
743 cumpolar Deep Water intrusions onto the Amundsen Sea continental shelf simulated

744 with an isopycnic coordinate ocean model. *Geophys. Res Letters*, **35**, L18 602, doi:
745 10.1029/2008GL034939.

746 Thompson, D. W. J. and S. Solomon, 2002: Interpretation of recent southern hemisphere
747 climate change. *Science*, **296 (5569)**, 895–9, doi:10.1126/science.1069270.

748 van den Broeke, M., 2005: Strong surface melting preceded collapse of antarctic peninsula
749 ice shelf. *Geophys. Res Letters*, **32 (12)**, L12 815, doi:10.1029/2005GL023247.

750 Wilchinsky, A. V. and D. L. Feltham, 2009: Numerical simulation of the filchner overflow.
751 *J. Geophys. Res.*, **114 (C12)**, C12 012, doi:10.1029/2008JC005013.

752 Williams, A., S. Bacon, and S. Cunningham, 2006: Variability of the lower circumpolar deep
753 water in drake passage 19262004. *Geophys. Res Letters*, **33 (3)**, L03 603, doi:10.1029/
754 2005GL024226.

755 Zwally, H. J., D. Yi, R. Kwok, and Y. Zhao, 2008: Icesat measurements of sea ice freeboard
756 and estimates of sea ice thickness in the weddell sea. *J. Geophys. Res.*, **113 (C2)**, C02S15,
757 doi:10.1029/2007JC004284.

758

List of Tables

TABLE 1. Drake Passage (SR1b) section details. Cruise numbers starting with JR were made on board RRS James Clark Ross and those starting with JC were made on board RRS James Cook. The batch number of the Standard Sea Water used for salinity calibration are given when available. SB: SeaBird, NBI: Neil Brown Instrument

Season	Start Date (yyyy/mo/dd)	Start Date (yyyy/mo/dd)	Ship/Cruise	CTD type	Thermometer	SSW batch
1993/94	1993/11/21	1993/11/26	JR0a	NBI MkIIIc	Reversing	P120, 123
1994/95	1994/11/15	1994/11/21	JR0b	NBI MkIIIc	Reversing	P123
1995/96	No cruise	-	-	-	-	-
1996/97	1996/11/15	1996/11/20	JR 16	NBI MkIIIc	Reversing	Unknown
1997/98	1997/12/29	1998/01/07	JR 27	NBI MkIIIc	Reversing	P132
1998/99	No cruise	-	-	-	-	-
1999/00	2000/02/12	2000/02/17	JR 47	SB 911 plus	SBE35	P132
2000/01	2000/11/22	2000/11/28	JR 55	NBI MkIIIc	Reversing	P136, 138
2001/02	2001/11/20	2001/11/26	JR 67	SB 911 plus	SBE35	P137, 139, 140
2002/03	2002/12/27	2003/01/01	JR 81	SB 911 plus	SBE35	P140
2003/04	2003/12/11	2003/12/15	JR 94	SB 911 plus	SBE35	P143
2004/05	2004/12/02	2004/12/08	JR115	SB 911 plus	SBE35	P143, 144
2005/06	2005/12/07	2005/12/12	JR139	SB 911 plus	SBE35	P144, 146
2006/07	2006/12/08	2006/12/12	JR163	SB 911 plus	SBE35	P144, 146
2007/08	2007/11/30	2007/12/05	JR193	SB 911 plus	No	P147
2008/09	2008/12/13	2008/12/18	JR194	SB 911 plus	SBE35	Unknown
2008/09	2009/02/20	2009/02/26	JC031	SB 911 plus	SBE35	P150
2009/10	2009/11/19	2009/11/26	JR195	SB 911 plus	SBE35	P150
2010/11	2010/11/19	2010/11/26	JR242	SB 911 plus	SBE35	Unknown
2010/11	2011/03/01	2011/03/07	JR276	SB 911 plus	SBE35	Unknown
2011/12	2011/11/28	2011/12/05	JR265	SB 911 plus	SBE35	Unknown

TABLE 2. Total ice loss by the LIS (top rows) and tributary glaciers (lower rows) based on published data (assuming density of ice is 900 kg m^{-3}). Ice shelf volume losses are estimated from the total volume losses for each ice shelf (Shepherd et al. 2010) distributed in time according to the ice-area losses (Scambos et al. 2003).

Period	Location	Total Ice loss (km^3)
1993	Gustav; LAIS	190 ± 40
1995	Gustav; LAIS; LBIS	950 ± 200
1998-2000	LBIS	740 ± 150
2002	LBIS	1000 ± 200
2001-2006	LBIS (Crane–Drygalski glaciers)	62 ± 14 (Shuman et al. 2011)
2006-2011	LBIS (Pequod–Hektoria)	50 ± 12(Berthier et al. 2012)
2003	LBIS (Leppard–Drygalski)	27 ± 9(Rignot et al. 2004)
2005	LBIS (Leppard–Drygalski)	34 ± 10 (Rignot 2006)
2008	LBIS (Pequod–Hektoria)	4 ± 2 (Rott et al. 2011)

List of Figures

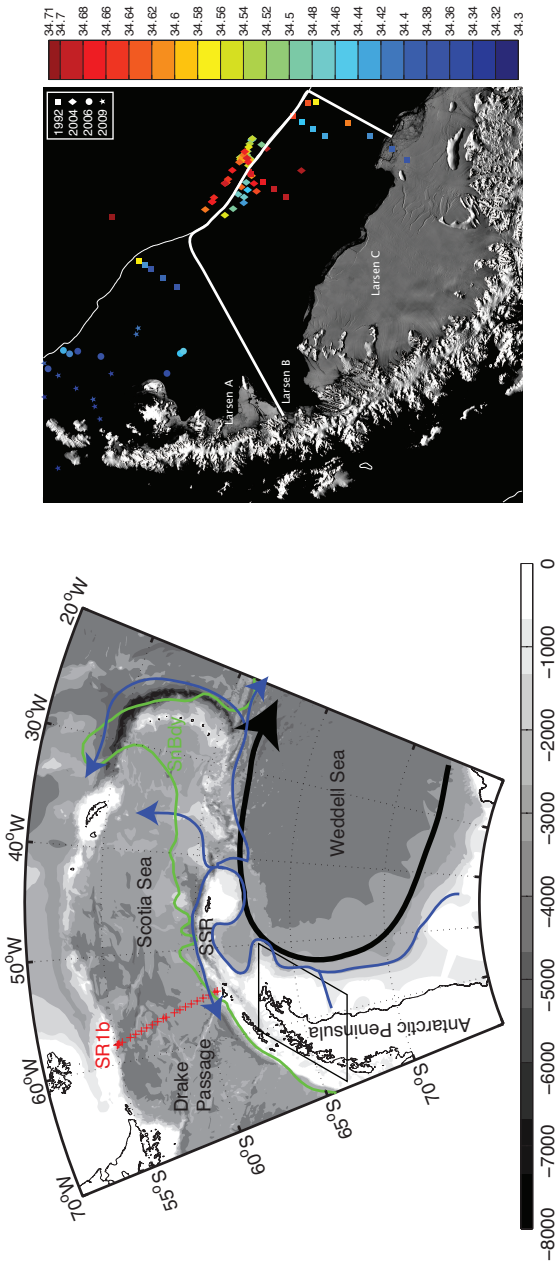

FIG. 1. a) Map of Drake Passage and SR1b station positions (in red). Schematic views of the Weddell Gyre (black) and AABW circulation (blue) are shown by the arrows. The southern boundary of the ACC (Orsi et al. 1995) is marked in green. The black box delineates the area of the map shown in Fig. 1b. SSR: South Scotia Ridge. b) MODIS Mosaic of Antarctica Image Map of the Antarctic Peninsula (corresponding to the black box in Fig. 1a) downloaded from the National Snow and Ice Data Center (http://nsidc.org/data/moa/index.html). The near-bottom salinity of hydrographic stations in the vicinity of the LIS is shown by the coloured circles. CTD data were obtained from the Pangaea web site (http://www.pangaea.de/) and include stations from the Ice Station Weddell, Winter Weddell Gyre Study, Ice Station Polarstern and ANT_X_7 cruises. The thin white line is the 1000m isobath and the thick white line delimits the shelf region where shelf waters are saline enough (Gill 1973) to contribute to AABW formation.

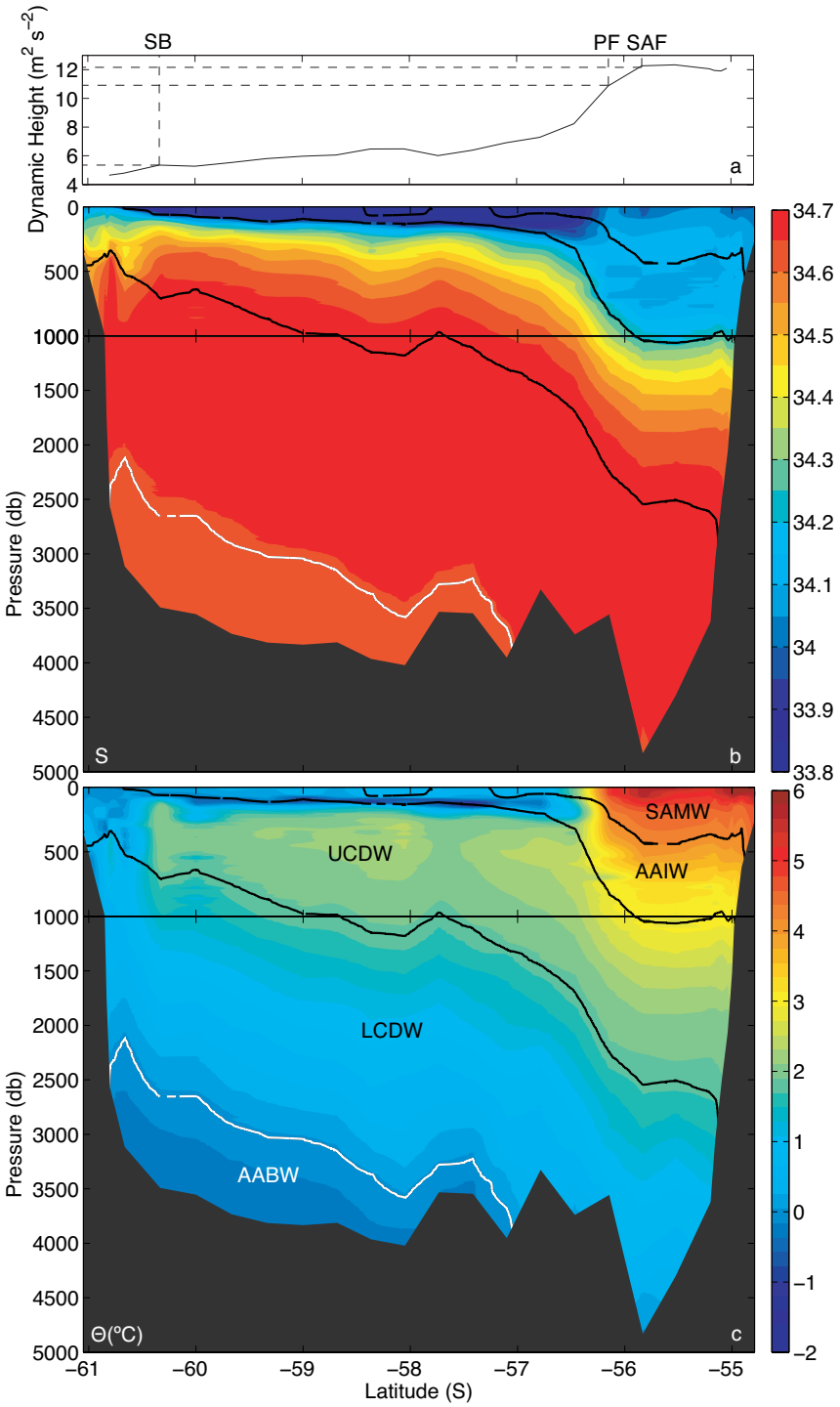

FIG. 2. (a) Dynamic height at 400 db relative to 2000 db. The positions of the main fronts of the Antarctic Circumpolar Current are indicated. SB: Southern Boundary; PF: Polar Front; SAF: Sub-Antarctic Front. Illustrative (b) potential temperature and (c) salinity distributions from the 2011/2012 SR1b section occupation. The neutral density (γ_n) limits of the main water masses are shown in black and the upper boundary of AABW ($\gamma_n = 28.26$ kg m^{-3}) is shown in white. SAMW: Sub-Antarctic Mode Water; AAIW: Antarctic Intermediate Water; UCDW: Upper Circumpolar Deep Water; LCDW: Lower Circumpolar Deep Water; AABW: Antarctic Bottom Water.

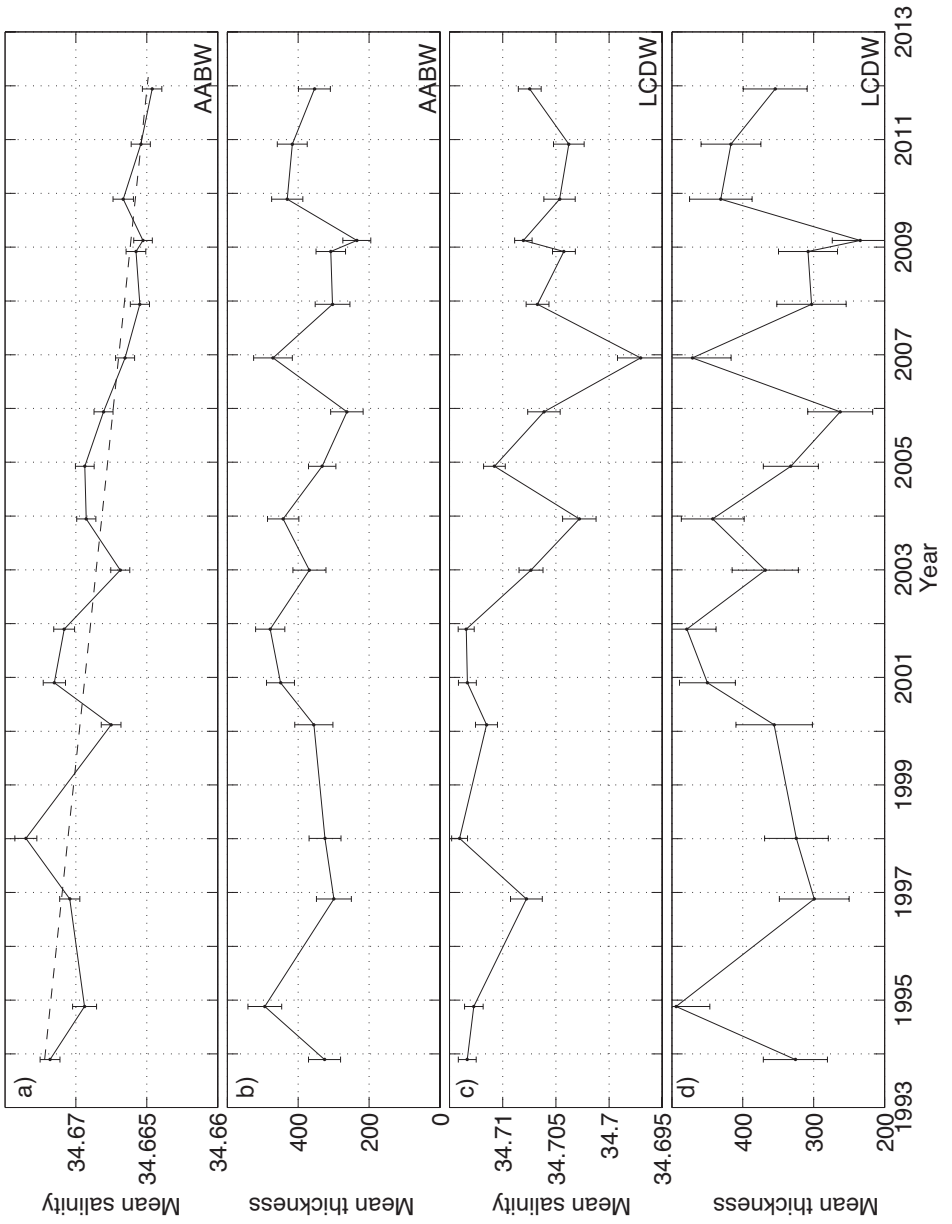

FIG. 3. Time series of the 18 Θ-salinity mean profiles of the AABW on the SR1b section gridded into dynamic height / neutral density space (see section 2). The profiles are color-coded as a function of year. The upper neutral density (γ_n) limit of AABW ($\gamma_n = 28.26$ kg m^{-3}) is shown. AABW is only present in the southernmost part of the SR1b section south of the Polar Front (Figure 2).

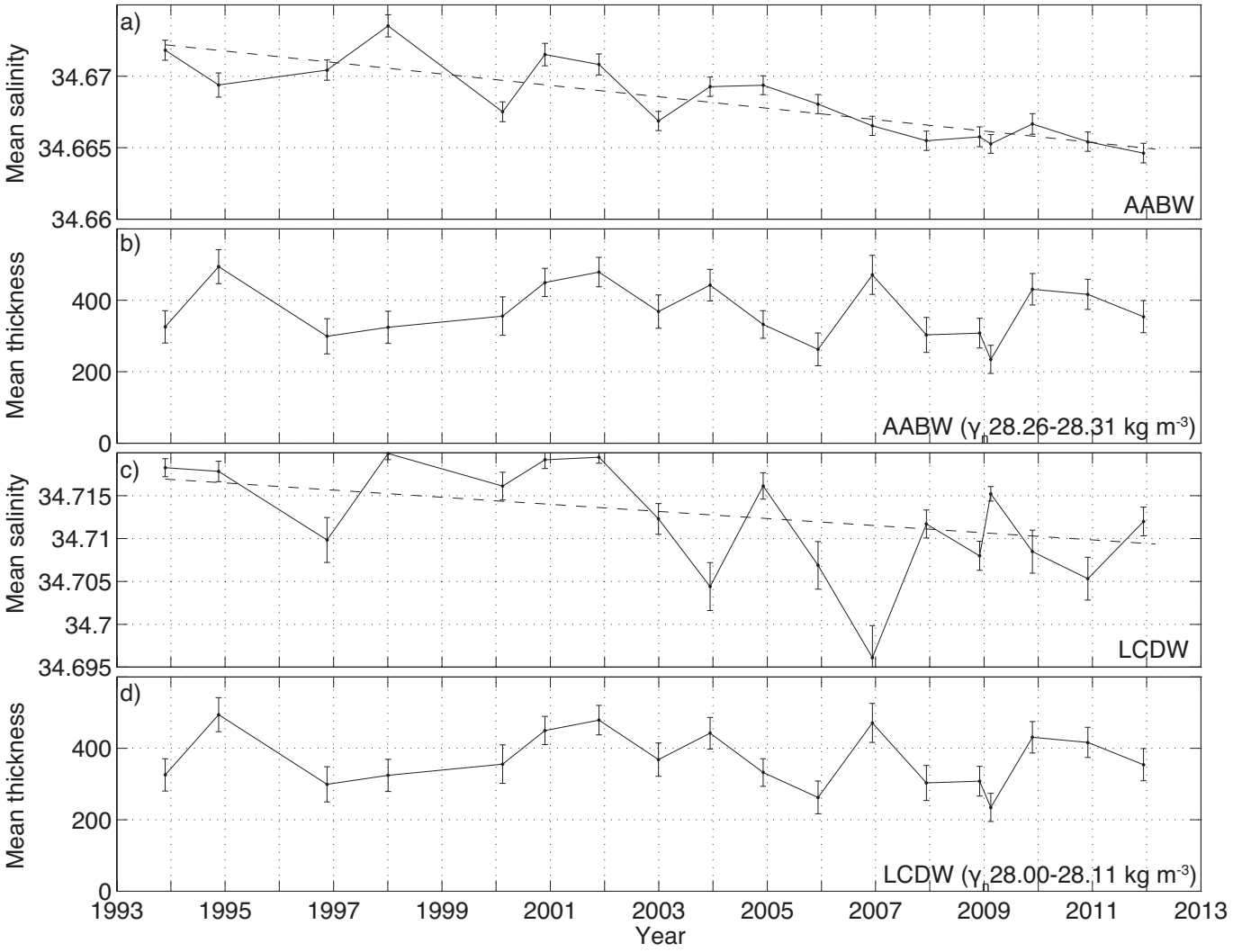

FIG. 4. Time series of a) salinity and b) layer thickness of the Antarctic Bottom Water ($\gamma_n = 28.26 - 28.31$ kg m^{-3}) on the SR1b sections. Time series of c) salinity and d) layer thickness of the Lower Circumpolar Deep Water ($\gamma_n = 28.00 - 28.26$ kg m^{-3}) on the SR1b sections. Linear trends of the salinity time series are shown by the dashed lines.Error bar on the mean salinity and thickness are shown as vertical bars (See Appendix for details on the error calculation).

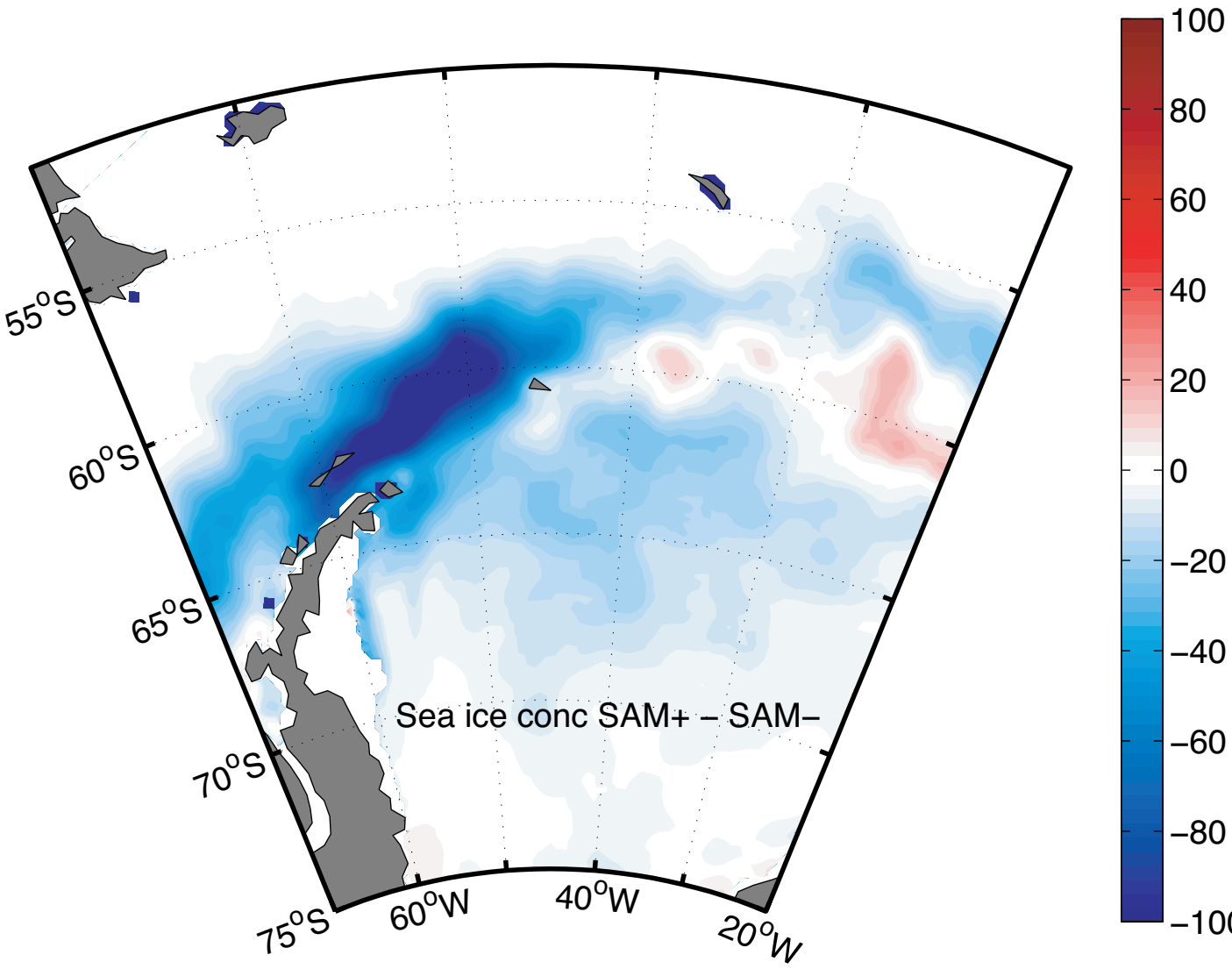

FIG. 5. Map of the correlation between the SR1b AABW salinity and the winter (JJA) sea ice concentration 18 months before in the western Weddell Sea. The black rectangle shows the location of the statistically significant correlation (at the 80% confidence level) off the LIS.